中正嶺學報 第三十三卷 第二期 民國 94.5.
JOURNAL OF C.C.I.T., VOL.33, NO.2, MAY, 2005

短文 Short Note

The Extraction and Reconstruction of the Generalized Evanescent Feature for the Texture Image: A Wavelet-Based Algorithm

Jiann-Ling Kuo[*], Taoi Hsu[**], Wen Liang Hwang[***] and Der-Kuo Tung[*]

[*]School of Defense Science, Chung-Cheng Institute of Technology , National Defense University
[**]Graphic Communication Technology Department, Shih Hsin University
[***]Institute of Information Science, Academia Sinica

ABSTRACT

In this paper, a wavelet-based algorithm is proposed to extract and reconstruct the generalized evanescent components of the texture image. This algorithm exploits the fact that the spectral properties of the generalized evanescent field have peaks distributed on lines of rational slope. When considering these line-like evanescent features as edges, the wavelet-based singularity detection theory can be used to accurately locate these features. The contributions of this paper are two folds. First, a novel algorithm is proposed to successfully handle the evanescent features. Second, the comparative review and experiment are presented to respectively show the effectiveness and efficiency of the three current Wold decomposition algorithms. It is shown from the experimental results that the proposed algorithm is more robust than the other two algorithms.

Keyword: evanescent feature, singularity detection, Wold decomposition, texture analysis

紋理影像一般性微差特徵之萃取與重建—小波轉換為基礎的演算法

郭劍凌[*] 徐道義[**] 黃文良[***] 董德國[*]

[*]國防大學中正理工學院國防科學研究所
[**]世新大學平面傳播科技學系
[***]中央研究院資訊科學研究所

摘要

在本研究中，我們提出了一個新的演算法，來處理紋理影像中一般性微差特徵之萃取與重建的問題。這個演算法運用了一般性微差子場的一個重要的頻域特性，那就是該子場在頻域中會有連續、密集但可數的峰值，這些峰值會分配在一些斜率為有理數值的直線上。因此，當把這些線狀型態的微差特徵視為邊線時，以小波為基礎的奇異性偵測理論便可以用來精確的找到這些特徵。本研究的貢獻有二：第一，提出了一個可靠的演算法可以成功地用來處理微差特徵。第二，對目前最新的三個華德分解演算法進行實驗與評估，以便分別比較它們的效率與有效性。由實驗的結果證實，本演算法較其他二演算法具有較佳的強健性。

關鍵詞: 微差特徵, 奇異性偵測, 華德分解, 紋理分析

文稿收件日期 91.12.12; 文稿修正後以短文接受日期 93.8.3.
Manuscript received Dec. 12, 2002; revised as short note Aug. 3, 2004.

I. INTRODUCTION

Texture characterization is still an important topic because many relevant 1D mathematical theories, while extending to 2D, remain open-questioned. In reference 1, the authors propose a multiresolution Lebesgue decomposition algorithm to extract and reconstruct the half plane deterministic component of texture image. In reference 2, the authors extend the theory and the algorithm in [1] to process the *generalized evanescent feature* of texture image. In this paper, the authors continue to propose another algorithm to extract and reconstruct the generalized evanescent components. The motivation behind is prepared to deeply understand the spectral peaks clustering on areas of “blob-like” or on curves of “multiple-pixel-wide” shape, which are considered as extending structures of generalized evanescent feature in the series of the research. The proposed algorithm is based on the fact that the spectral properties of the generalized evanescent field have peaks distributed on lines of rational slope. These peaks are represented by the form of a countable sum of 1D delta functions which are singular and continuous along the lines of rational slope. They are also modulated by 1D purely indeterministic process from the orthogonal dimension.

To properly extract the generalized evanescent components, Francos et al. firstly elaborated the theory of 2D Wold decomposition [2]. With the theoretic analysis and exploration, they further proposed an algorithm to extract generalized evanescent component. Their algorithm uses periodogram as a frequency estimator and detects the component by choosing the frequencies of the peaks forming “continuous” lines.

In reference 4, Francos et al. further employ the maximum likelihood estimation (MLE) approach, which is presented in [5], to analysis and estimate texture image. This approach assumes, in 2D Wold decomposition model, the innovation field of purely indeterministic component is Gaussian and from which the likelihood function is derived. Then, by complicated derivation and transformation, the problem of maximization likelihood estimation can be achieved by minimizing a less complex but nonlinear objective function which consists of only the harmonic and evanescent component spectral support parameters. Due to the non-linearity of the objective function, however, the minimization problem has to be solved by numerical method. According to their 2-stage numerical method, a sub-optimal initial estimate for the parameters of the objective function is obtained firstly. Then, a line-search conjugate gradient method is applied to refine the initial estimates.

To ameliorate the problem of high computational burden, Francos further derives a new algorithm for estimating the parameters of the evanescent and purely indeterministic components [6]. This algorithm utilizes a nonlinear operator called evanescent to exponential transform (EET) to map each evanescent component to a single exponential

and make the problem of estimating the spectral support parameters of the evanescent component become the estimation of the spatial frequency of a 2D exponential function. Then, the first step of the 2-stage numerical method in [5] can be replaced by this EET-based algorithm to obtain the initial estimate of the parameters. In fact, this EET transformation is an autocovariance function. By using the sample unconjugated second-order moment, an autocovariance estimate of the random field is obtained. This autocovariance estimate is then Fourier-transformed to further obtain the power spectral density (PSD) estimate of the field. Since the evanescent component consisting of a 1D harmonic process modulated by a 1D purely indeterministic process, the PSD function of the evanescent field can be characterized by a singular function which consists of 1D dirac function that are countable and continuous along the support line and singular in the orthogonal dimension. Thus, by searching the prominent peaks in the PSD estimate of the field, the number and the spectral support parameters of evanescent component can be initially estimated.

Based on the theoretic structure of [3], Liu and Picard propose a new decomposition algorithm to separate a texture image [7,8]. In their algorithm, the generalized evanescent component is extracted by utilizing the Hough transform of the Fourier magnitude image which is the scaled square root of the periodogram. The most important information of their algorithm are the number of local maximum in polar plane histogram of Hough transform for generalized evanescent field. If these information are chosen insufficiently, some structural components will be lost. On the contrary, part of the purely indeterministic component will be selected and make the extraction of the generalized evanescent component over-determinant. Unfortunately, from [7-9] and relevant documentation, they did not describe the mechanism of how to obtain these information. This will affect the robustness of their algorithm.

From the above description, a mainly conclusion to be made is that the number of the generalized evanescent components and the accurate position of their frequency support can not be properly and simultaneously obtained or can only be partially obtained by these current algorithms. This is the same problem as the "*what is where*?" question [10]. However, in this research, the authors propose a novel algorithm which can properly obtain both the "what" and "where" information at the same time to resolve these problems.

This paper is organized as follows. Section II presents the texture model and the spectrum used for this research. Followed is the proposed algorithm for the extraction and reconstruction of the generalized evanescent feature. Section IV demonstrates and compares the experimental results. Finally, the conclusion and future work are given.

II. THE TEXTURE MODEL AND THE SPECTRUM OF THE TEXTURE IMAGE

Following the results in [2], the model adopted in this paper is as following:

$$y(n,m)=\xi(n,m)+e(n,m)=\xi(n,m)+\sum_{(\alpha,\beta)\in O} e_{(\alpha,\beta)}(n^{(\alpha,\beta)},m^{(\alpha,\beta)})$$

$$=\sum_{(0,0)\le(k,l)} a(k,l)\varepsilon(n-k,m-l)+$$

$$\sum_{(\alpha,\beta)\in O}\sum_{t=1}^{p}[B_t^{(\alpha,\beta)}(n^{(\alpha,\beta)})\cdot\cos(v_t^{(\alpha,\beta)}\cdot m^{(\alpha,\beta)}+\psi_t^{(\alpha,\beta)})] \quad (1)$$

To thoroughly extract all possible evanescent components, most of the current algorithms are designed to estimate the possible co-prime pairs, $(\alpha,\beta)s$, in advance. After that, in each possible (α,β), the other parameters are estimated accordingly. However, the reader can find from latter sections that the proposed algorithm can extract all possible evanescent components without estimating (α,β) pairs. This is one of the contributions for this research.

The integrated spectrum of $y(n,m)$, denoted by $F_y(\mu,\eta)$, can be expressed as:

$$F_y(\mu,\eta)=F_\xi(\mu,\eta)+F_e(\mu,\eta). \quad (2)$$

$F_\xi(\mu,\eta)$ and $F_e(\mu,\eta)$ are respectively the integrated spectrum of $\xi(n,m)$ and $e(n,m)$, where $F_e(\mu,\eta)=\sum_{(\alpha,\beta)\in O} F_{e_{(\alpha,\beta)}}(\mu^{(\alpha,\beta)},\eta^{(\alpha,\beta)})$ and $F_{e_{(\alpha,\beta)}}(\mu^{(\alpha,\beta)},\eta^{(\alpha,\beta)})$ is the integrated spectrum computed in the (α,β) RNSHP support. And,

$$F_\xi(\mu,\eta)=\int_{-\pi}^{\mu}\int_{-\pi}^{\eta} P_\xi(\theta_1,\theta_2)d\theta_1 d\theta_2 \quad (3)$$

$$F_{e_{(\alpha,\beta)}}(\mu^{(\alpha,\beta)},\eta^{(\alpha,\beta)})=\int_{-\pi}^{\mu^{(\alpha,\beta)}}\int_{-\pi}^{\eta^{(\alpha,\beta)}} P_{e_{(\alpha,\beta)}}(\theta_1,\theta_2)d\theta_1 d\theta_2 \quad (4)$$

where

$$P_\xi(\mu,\eta)=\frac{\sigma^2_{\varepsilon(n,m)}}{(2\pi)^2}\left\{\sum_{\tau_n=-\infty}^{\infty}[\theta(\tau_n,0)+\Lambda(\tau_n)]e^{-i\mu\tau_n}\right\}+$$

$$\frac{\sigma^2_{\varepsilon(n,m)}}{2\pi^2}\left\{\sum_{\tau_n=-\infty}^{\infty}\sum_{\tau_m=1}^{\infty}[\theta(\tau_n,\tau_m)+\Lambda(\tau_n)]e^{-i(\mu\tau_n+\eta\tau_m)}\right\}; \quad (5)$$

$$P_{e_{(\alpha,\beta)}}(\mu^{(\alpha,\beta)},\eta^{(\alpha,\beta)})=\frac{1}{(4\pi)^2}\sum_{t=1}^{p}\{P_{B_t^{(\alpha,\beta)}}(\mu^{(\alpha,\beta)})\cdot$$

$$[\delta(\eta^{(\alpha,\beta)}+v_t^{(\alpha,\beta)})+\delta(\eta^{(\alpha,\beta)}-v_t^{(\alpha,\beta)})]\}. \quad (6)$$

$\sigma^2_{\varepsilon(n,m)}$ is the 2D noise variance, p is the number of the evanescent components in the (α,β) RNSHP support, τ_n and τ_m are shifts in abscissa and ordinate respectively and

$$\theta(\tau_n,\tau_m)=\sum_{l=0}^{m-\tau_m} a(0,l)a(\tau_n,M-1-(m-\tau_m-l)); \quad (7)$$

$$\Lambda(\tau_n)=\sum_{k=1}^{n-\tau_n}\sum_{l=0}^{M-1} a(k,l)a(\tau_n+k,l). \quad (8)$$

The derivation of the above equations can be found in Ref. 2. And as in [2], the proposed algorithm is designed to decompose

the PSD function $\sum_{(\alpha,\beta)\in O} P_{e_{(\alpha,\beta)}}(\mu^{(\alpha,\beta)},\eta^{(\alpha,\beta)})$ instead of the spectrum $\sum_{(\alpha,\beta)\in O} F_{e_{(\alpha,\beta)}}(\mu^{(\alpha,\beta)},\eta^{(\alpha,\beta)})$.

III. THE PROPOSED ALGORITHM FOR EXTRACTION AND RECONSTRUCTION OF THE GENERALIZED EVANESCENT FEATURE

From the above description, it can be easily found that the spatial property of the generalized evanescent field can be considered as system of waves all traveling in the same direction, while the spectral property of the field can be described by a countable sum of dense spectral peaks supported on lines of rational slope[3]. In this section, the algorithm for the generalized evanescent field is proposed to tackle the extraction and reconstruction problem for the field. This algorithm is classified as a frequency-domain-oriented method.

To separate the evanescent field from purely indeterministic one, the position and content information of this field should be obtained in advance. This is a same problem as the "*What is where*?" question [10]. Especially, when this field is embedded in the purely indeterministic one, it is often not easy to distinguish the former from the latter. Fortunately, the multiresolution framework provides an excellent mechanism. In this framework, the spectral image is firstly analyzed at a coarse resolution to obtain the more reliable "what" content information such as peak classes in spectral analysis. This information is then propagated by using the coarse-to-fine strategy to guide the effective searching of the "where" position information. As is well known, singularities are important features in image. To accurately locate the position of the wanted singularities is always a key topic in many kind of research. From the description of the evanescent field's spectral property, it can be characterized as lots of singularities distributed along lines of rational slope. In Ref. 11, Tang *et. al*. show that the local modulus maximum of the wavelet transform with respect to these lines are slope invariant, gray-level invariant and width light-dependent. This provides a constructive suggestion that wavelet transform is an ideal tool to analyze these singularity lines.

To extract the generalized evanescent feature $\sum_{(\alpha,\beta)\in O} P_{e_{(\alpha,\beta)}}$ from PSD P_y, some parameter estimation procedures for estimating functions $\theta(\tau_n,\tau_m)$ and $\Lambda(\tau_n)$ and the parameters in $B_t^{(\alpha,\beta)}$ should be accomplished in advance. However, in order to quickly demonstrate the feasibility of the theory mentioned in last subsection, the texture's Fourier magnitude which is the scaled square root of the periodogram is used as the estimator. Based on this estimator, the proposed algorithm can be conducted properly. This is the same estimator used in [3] and [7]. And from this basis, the proposed algorithm

can be fairly compared to that in [3] and [7]. Also, to clearly illustrate the algorithm, an evanescent texture pattern is given in Fig. 1 for description convenience. This pattern is the Brodatz texture D94. The algorithm is similar to that of [12] in which one of the authors use a similar method to extract characters from documents in the OCR application. However, in that application, the characters are considered as the darkest gray value in the document, which simplifies the extraction problem.

In the first step of the algorithm, the texture is zero-meaned and its Fourier magnitude is computed as in Fig. 1(b). Then, the multiresolution analysis is applied to the Fourier magnitude. When combining this technique to the Lebesgue decomposition of $P_y(\mu,\eta)$ which consists of an absolutely continuous $P_\xi(\mu,\eta)$ and a singular part $P_e(\mu,\eta)$ as defined in Eqs. (5) and (6), $P_\xi(\mu,\eta)$ will be smoothed and $P_e(\mu,\eta)$ will remain dominant at coarse resolution. To accomplish this analysis step, four sub-steps are implemented. First, the modulus maximum is computed at each scale. Second, to properly locate these "continuous singularities", some kind of linking procedure should be involved. Recall that the horizontal

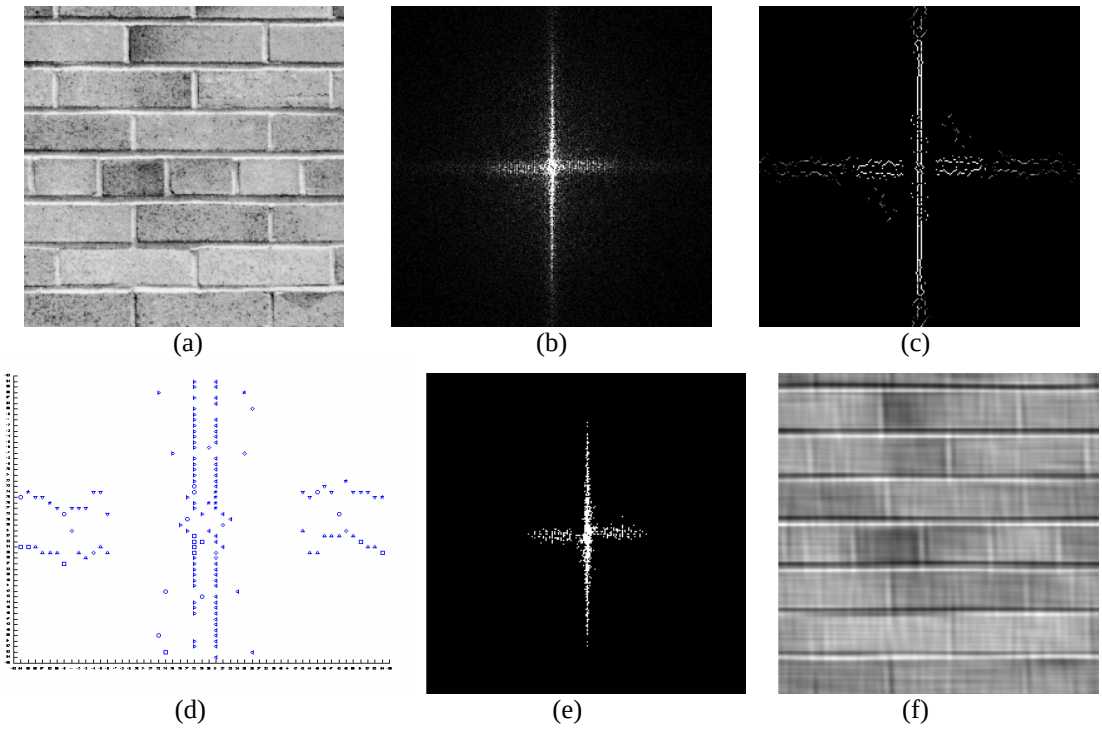

Fig 1. Evanescent feature extraction of Brodatz texture D94. (a) the original image; (b) its spectrum image; (c) edge position information detected at finer scale; (d) the direction information of the central part of (c); (e) the detected evanescent spectral peaks; (f) the reconstructed evanescent component

and vertical components of the wavelet transform can be used to estimate the gradient vector of a function. In fact, the modulus maxima of the wavelet transform do representa local maximum in the direction of the gradient. Thus, by linking these modulus maxima at each scale, the position information of the singularity curves can be properly handled. Because the modulus maximum represents the length of the gradient vector at a point, it is the maximum rate of change between that point and its neighbors. To link these modulus maxima at a scale s, all we have to do is to find out the similar argument $AP_y(s,\mu,\eta)$ from the neighbors of point (μ,η) at scale s, with the minimum difference of magnitude between (μ,η) and its neighbors. Third, a thresholding technique is applied at coarse scale to remove those singularities considered as trivial. In practice, scale 2^3 is selected. The threshold value is set at $100-\alpha th$ percentile of the modulus at coarse scale. Fourth, the linked singularities at coarse scale are proposed to the finest scale 2^1 to obtain the more accurate edge position information. These four sub-steps accomplish the "what is where" mechanism as mentioned in last subsection. The result after this step is presented in Fig. 1(c).

In the following step, the argument information, i.e., the direction of the gradient vector, accompanied with the edge position information, are used to search for the wanted singularities inside the closed edge or between edges. This kind of direction information is shown in Fig. 1(d). There are 8 directions defined in this research. The symbols in Fig. 1(d) represent these directions they point to, e.g., "▷" points to the east; "▽" to the south; "◁" to the west; "△" to the north; "O" to the south-east; "☆" to the south-west; "□" to the north-east; and "◇" to the north-west. From this direction information, it can be easily found that the singularity features are all enclosed in or between these edges. For each pixel in every detected edges, we start searching according to its gradient vector direction. The stop condition for searching is that an opposite direction of the other gradient vector or an outer boundary of the image is encountered. To extract these evanescent features, we just search in or between edges in the Fourier magnitude image where the magnitude is grater than the median. The feasibility of this step is based on the fact that the direction of the gradient vector in the neighborhood of the singularity is always pointing to the local maximum of the singularity. The result for this step is demonstrated in Fig. 1(e).

At last, the singularities detected in Fig. 1(e) are used as the parameter set to characterize the evanescent component. The selected evanescent peaks in the Fourier spectrum are then inverse Fourier transformed to reconstruct the component. The reconstructed result is presented in Fig. 1(f). The overall algorithm is presented in table 1.

Furthermore, there is one point worthy to be mentioned. That is, it is not necessary to

Table 1. The proposed algorithm

The algorithm:

Step1. Zero-mean the texture image and compute its Fourier magnitude.
Step2. Multiresolution analysis of the Fourier magnitude image using 2D dyadic wavelet transform in [13].
Step2.1 Compute the modulus maximum at each scale.
Step2.2 Link the singularities along curves of possible edges.
Step2.3 Threshold at coarse scale. The threshold value is set at $100\,\alpha$ -th percentile of the modulus at scale 2^3.
Step2.4 Position information propagation. Propagate the "what" information obtained at coarse scale to the finer scale.
Step3. Use the edge position information obtained in step 2.4 with the relevant direction information to search for the wanted evanescent singularities inside the closed edge or between edges. The searching criterion is set at the median of the original Fourier magnitude. The amplitudes greater than this criterion are chosen as the wanted singularities.
Step4. Reconstruction of the evanescent component.

estimate the parameter pair, (α, β) in this algorithm. This is because the proposed algorithm treats the line-like evanescent features as edges. And the edge with different direction can be detected simultaneously. For example, $(\alpha, \beta) = (0,1)$ means a horizontal evanescent component while $(\alpha, \beta) = (1,0)$ represents a vertical one. Both of these features can be detected as in Fig. 1(e).

IV. EXPERIMENTAL RESULTS AND COMPARISON

In this section, a series of experiment have been conducted to demonstrate the effectiveness and efficiency of the proposed algorithm. Generally speaking, the current decomposition algorithm can be classified into two categories: time-time-domain-oriented and frequency-domain-oriented. Until now, the only one time-domain-oriented algorithm is the MLE method proposed by [5]. Since the decomposition algorithm of this type is very complicated and computationally expensive and since the proposed algorithm belong to the frequency-domain-oriented category, the comparisons will be focused on the frequency-domain-oriented method. That is, the experiment results of the proposed algorithms are compared to that of the other two algorithms in [3] and [7] which are reviewed in section one.

The texture images used in these experiments are Brodatz texture [14] and synthetic texture. These texture images are selected as versatile as possible to

make the experiment more objective. The size of these texture image are all 256×256. Figures 2~4 use the natural Brodatz texture D64, D78 and D94, while Fig. 5 and Fig. 6 use the synthetic texture. The first synthetic texture image S1, as shown in Fig. 5(a), is synthesized by a 1D sinusoidal function modulated by a 1D moving average process of order 2. The 1D sinusoidal function has 5 different frequency components characterized by vector [0.1 0.3 0.5 0.7 0.9]. The 1D moving average model is adopted from [15] with the form of $\xi(n) = \varepsilon(n) + 1.1 \cdot \varepsilon(n-1) + 0.2 \cdot \varepsilon(n-2)$. The second synthetic texture image S2, as shown in Fig. 6(a), is synthesized by a 2D sine-grating function superimposed with a 2D moving average process. The 2D sine-grating function has 2 different frequency component respectively characterizing the upper half and lower half of the 2D plane. And the 2D moving average process is extended from the above 1D case with NSHP order definition. From these experiment results, some comparative conclusion can be easily drawn. In the algorithm of [3], since there is no objective criterion in selecting the sharp and large-amplitude spectral peaks, the number of the evanescent peaks detected by the proposed algorithm is taken as a reference. That is, in the above experiments, the number of the evanescent peaks extracted by the

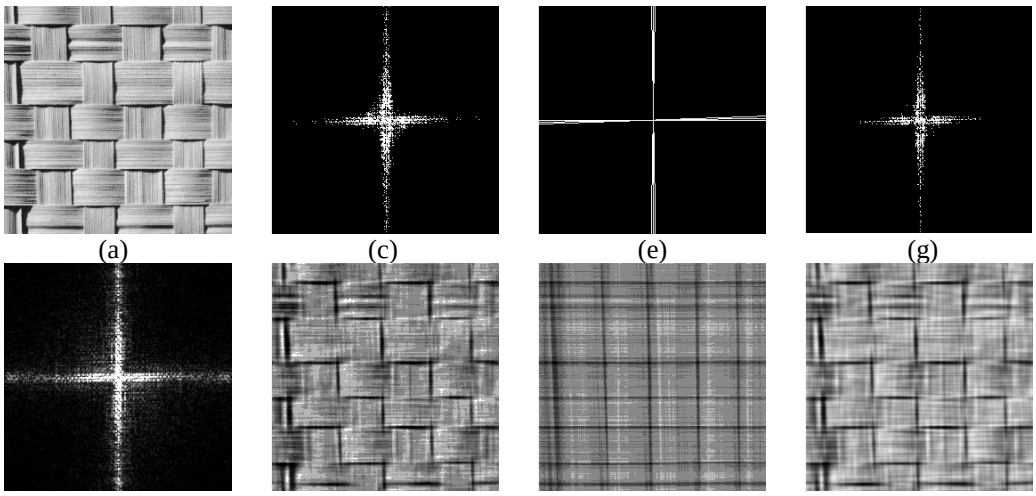

Fig.2 Evanescent feature extraction and reconstruction of Brodatz texture D64. (a)original image; (b)its spectrum image；(c)peaks detected by the algorithm of [3]；(d)evanescent reconstructed from the peaks in (c)；(e) peaks detected by the algorithm of [7]；(f)evanescent reconstructed from the peaks in (e)；(g)peaks detected by the proposed algorithm；(h) evanescent reconstructed from the peaks in (g).

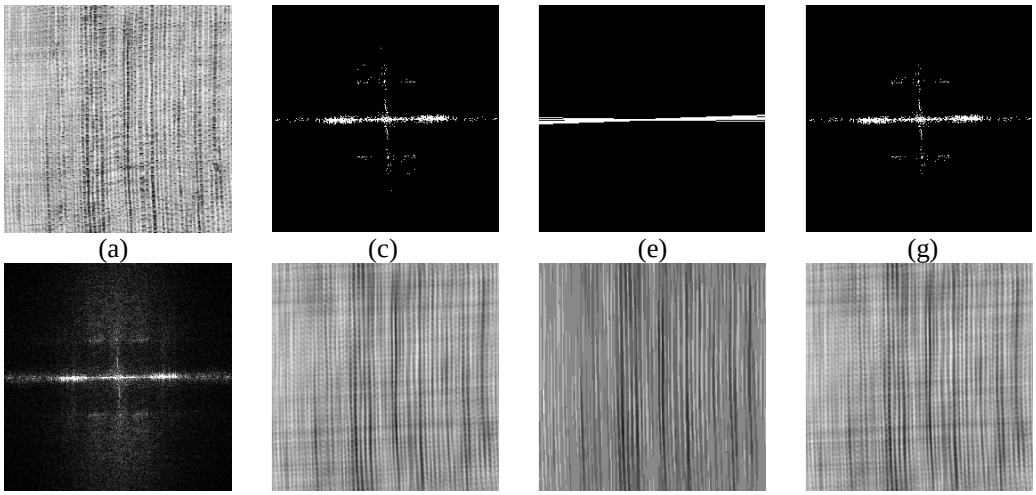

Fig.3 Evanescent feature extraction and reconstruction of Brodatz texture D78. (a)original image; (b)its spectrum image；(c)peaks detected by the algorithm of [3]；(d)evanescent reconstructed from the peaks in (c)；(e) peaks detected by the algorithm of [7]；(f)evanescent reconstructed from the peaks in (e)；(g)peaks detected by the proposed algorithm；(h) evanescent reconstructed from the peaks in (g).

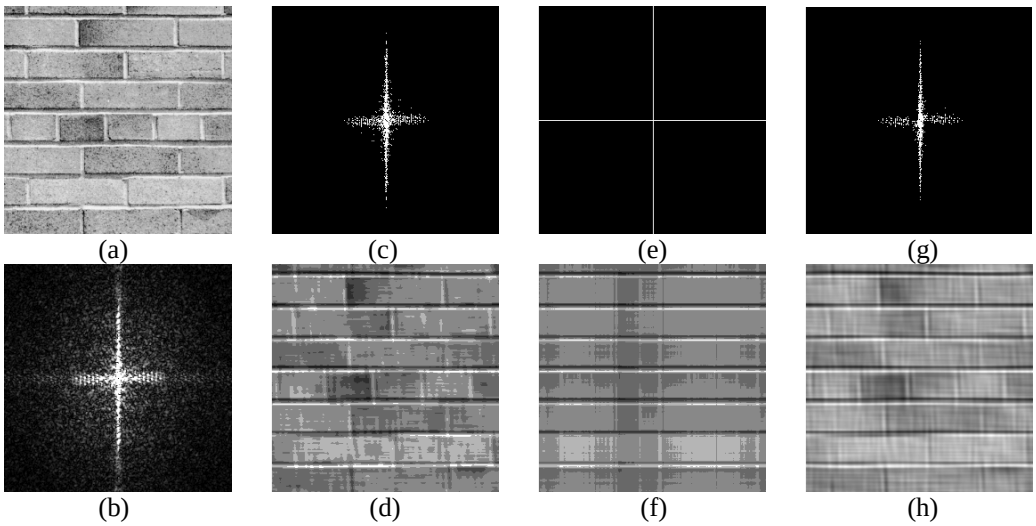

Fig.4 Evanescent feature extraction and reconstruction of Brodatz texture D94. (a)original image; (b)its spectrum image；(c)peaks detected by the algorithm of [3]；(d)evanescent reconstructed from the peaks in (c)；(e) peaks detected by the algorithm of [7]；(f)evanescent reconstructed from the peaks in (e)；(g)peaks detected by the proposed algorithm；(h) evanescent reconstructed from the peaks in (g).

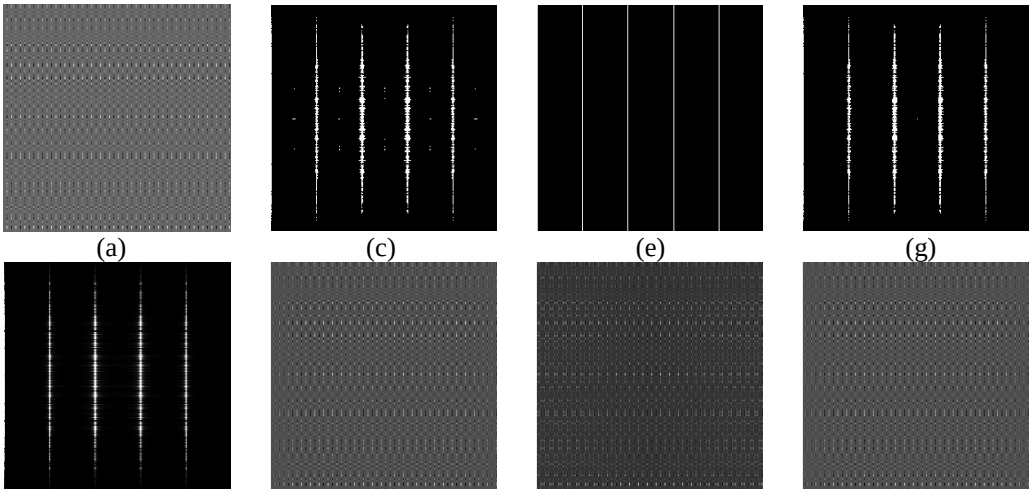

Fig.5 Evanescent feature extraction and reconstruction of synthetic texture S1. (a)original image; (b)its spectrum image；(c)peaks detected by the algorithm of [3]；(d)evanescent reconstructed from the peaks in (c)；(e) peaks detected by the algorithm of [7]；(f)evanescent reconstructed from the peaks in (e)；(g)peaks detected by the proposed algorithm；(h) evanescent reconstructed from the peaks in (g).

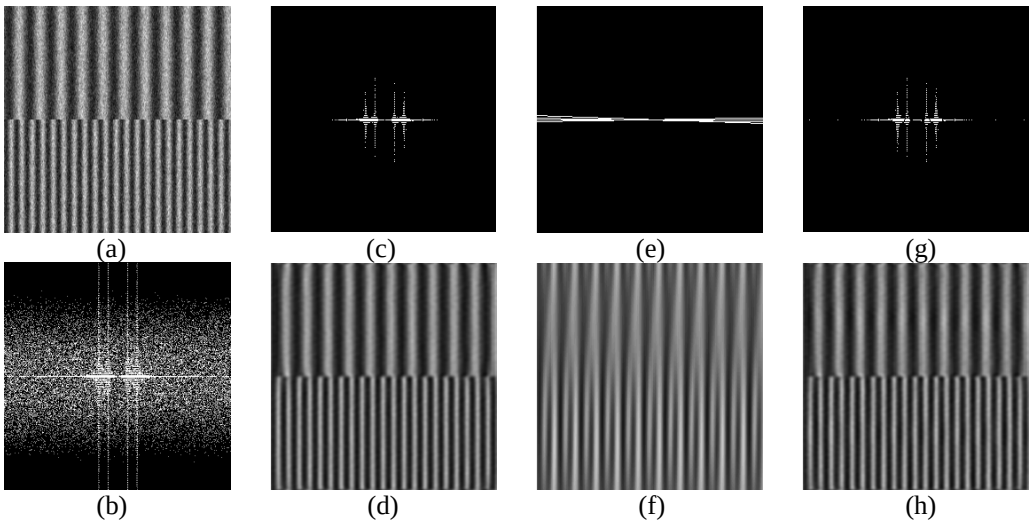

Fig.6 Evanescent feature extraction and reconstruction of synthetic texture S2. (a)original image; (b)its spectrum image；(c)peaks detected by the algorithm of [3]；(d)evanescent reconstructed from the peaks in (c)；(e) peaks detected by the algorithm of [7]；(f)evanescent reconstructed from the peaks in (e)；(g)peaks detected by the proposed algorithm；(h) evanescent reconstructed from the peaks in (g).

algorithm of [3] and the proposed algorithm are the same but with different distributed position. If the number of the evanescent peaks is not properly decided, the reconstruction results from algorithm of [3] will become unstable. This explains why the reconstruction results in Figs. 2(d)、3(d)、4(d)、5(d) and 6(d) look as good as those in Figs. 2(h)、3(h)、4(h)、5(h) and 6(h) respectively. The less number of the evanescent singularities extracted by the algorithm of [3], the poor results will be reconstructed.

From these figures, it can easily be found that the results detected by the algorithm of [3] are spread over the areas with some away from the evanescent lines, which pick up more purely indeterministic components. This can be shown from Figs. 2(c), 3(c) and 5(c). In addition, to detect all evanescent components, all possible (α, β) values have to be estimated. This needs extra procedure to accomplish and make the whole algorithm more complicated. Similarly, the results by the algorithm of [7] are generally unstable and dissatisfactory. This is because of the hard decision for the number of local maxima in Hough space. It is the same as to estimate (α, β) parameters. Besides, since the image size and the amplitude of purely indeterministic component will affect the geometric distribution of evanescent components, Hough transform is not suitable for the detection of evanescent line with rational slope.

As to the proposed algorithm, although it's a periodogram-based algorithm, the scaled square root periodogram (i.e., the texture's Fourier magnitude) is smoothed by a series of filters in the dyadic wavelet transform. This makes the estimation consistent. In the meantime, because the proposed algorithm is designed to detect edge, all possible edges in a spectrum image can be extracted within a single run. Thus, it is not necessary to estimate (α, β) parameters. In addition to the evanescent line with rational slope, the algorithm is suitable for even the evanescent peaks clustering on curves. And this is the main issue in another research. Furthermore, due to the multiresolution framework, it can always be found that the evanescent structure dominated in the coarse resolution, which automatically presents the position and the number of evanescent components. And this happens to ameliorate the mainly drawbacks of algorithms by [3] and [7]. Therefore, all of these comparisons demonstrate the robustness of the proposed algorithm.

V. CONCLUSION AND FUTURE WORK

In this paper, a wavelet-based Wold decomposition algorithm is proposed to extract evanescent components of the texture image. This algorithm is intended

to improve the current frequency-domain-oriented Wold decomposition algorithms that either overestimate or underestimate the evanescent components. The improvement is accomplished by the wavelet-based singularity detection theory of [16]. Although this theory is not suitable for directly processing texture image as claimed by its authors, with Lebesgue decomposition theory, the situation is totally changed.

Under the multiresolution framework, the evanescent feature can always be found dominated at coarse scale. After thresholding the trivial indeterministic component at coarse scale, the position information can then be propagated up to the finer scale to increase the accuracy of the position. Then, with the relevant sign information, the evanescent components can be properly extracted from scale 2^0. This is the main theme of this algorithm.

The contributions of this paper are three folds. The first is that the mathematical foundation used to handle the evanescent features is found. Based on this foundation, a novel algorithm is proposed to demonstrate its feasibility. And this is the second contribution. The third is that the comparative review and experiment are presented to respectively show the effectiveness and efficiency of the three current Wold decomposition algorithms.

From the experiments, the proposed algorithm can always obtain the satisfactory results that ensure its robustness and efficiency. However, as is well known, the performance of the periodogram-based algorithm are limited to the resolution constrain of the discrete Fourier transform. Also, there are other important issues, such as spectral peaks clustering on areas of “blob-like” or curves of “multiple-pixel-wide” shape, which are necessary to be considered. This inspires the authors to initiate another method to tackle this problem.

VI. REFERENCES

[1] Kuo, J. L., Hsu, T., Hwang, W. L., and Tung, D. K., “A Multiresolution Lebesgue Decomposition Algorithm for Extracting Harmonic Feature of Texture Images,” Journal of CCIT, Vol.31, No.1, pp. 93-112, 2002.

[2] Hsu, T., Hwang, W. L., Kuo, J. L., and Tung, D. K., “A Novel Wold Decomposition Algorithm for Extracting Deterministic Features from Texture Images:With Comparison,” IEICE Trans. on Fundamentals of Electronics, Communications and Computer Sciences, Vol.E87-A, No. 4, pp. 875-887, 2004.

[3] Francos, J. M., Zvi Meiri, A., and ,B., “A Unified Texture Model Based on a 2-D Wold-Like Decomposition,” IEEE Trans. on Signal Processing, Vol. 41, No. 8, pp. 2665-2678, 1993.

[4] Francos, J. M., Narasimhan, A., and

Woods, J. W., “Maximum Likelihood Parameter Estimation of Textures Using a Wold-Decomposition Based Model,” IEEE Trans. on IP, Vol.4, No. 12, pp. 1655-1666, 1995.

[5] Francos, J. M., Narasimhan, A., and Woods, J. W., “Maximum-Likelihood Parameter Estimation of Discrete Homogeneous Random Fields with Mixed Spectral Distributions,” IEEE Trans. on Signal Processing, Vol. 44, No.5, pp. 1242-1255, 1996.

[6] Francos, J. M., “The Evanescent Field Transform for Estimating the Parameters of Homogeneous Random Fields with Mixed Spectral Distributions,” IEEE Trans. on Signal Processing, Vol. 47, No. 8, pp. 2167-2180, 1999.

[7] Liu, F. and Picard, R. W., “Periodicity, Directionality, and Randomness: Wold Features for Image Modeling and Retrieval,” IEEE Trans. on PAMI, Vol. 18, No. 7, pp. 722-733, 1996.

[8] Liu, F. and Picard, R. W., “A Spectral 2D Wold Decomposition Algorithm for Homogeneous Random Fields,” Proceedings of the IEEE international Conference on Acoustics, Speech, and Signal Processing, Vol. 6, pp. 3501-3504, 1999.

[9] Liu, F., *Modeling Spatial and Temporal Textures*, PhD Thesis, School of Architecture and Planning, Massachusetts Institute of Technology, Cambridge, 1997.

[10] Marr, D., Vision, San Francisco, Freeman, 1982.

[11] Tang, Y. Y., Yang, L. and Liu, J., “Characterization of Dirac-Structure Edges with Wavelet Transform,” IEEE Trans. on SMC-Part B: Cybernetics, Vol. 30, No. 1, pp. 93-109, 2000.

[12] Hwang, W. L. and Chang, F., “Character Extraction from Documents Using Wavelet Maxima,” Image and Vision Computing, Vol. 16, pp. 307-315, 1998.

[13] Mallat, S. and Zhong, S., “Characterization of Signal from Multiscale Edges,” IEEE Trans. on PAMI, Vol. 14, No. 7, pp. 710-732, 1992.

[14] Brodatz, P., Textures: A Photographic Album for Artists and Designers, New York: Dover, 1966.

[15] Priestley, M. B., Spectral Analysis and Time Series, Vol. I and II, Academic Press, London, 1981.

[16] Mallat, S. and Hwang, W. L., “Singularity Detection and Processing with Wavelets,” IEEE Trans. on IT, Vol. 38, No. 2, pp. 617-643, 1992.